Implementation of a Phase Field Method in OpenFOAM® for Simulation of Spreading Droplets and Verification by Test Problems

Xuan Cai, Martin Wörner, Olaf Deutschmann

Institute of Catalysis Research and Technology, Karlsruhe Institute of Technology,
Hermann-von-Helmholtz-Platz 1, 76344 Eggenstein-Leopoldshafen, Germany

Email: xuan.cai@kit.edu

Keywords: Phase Field Method, OpenFOAM®, Moving Contact Line, Droplet Spreading

Abstract

In this work, we present the implementation of a phase field method in OpenFOAM® for simulation of spreading phenomena involving moving contact lines. The method is verified and validated by several one-dimensional and two-dimensional test problems and the influence of various numerical parameters is investigated. A critical issue is the diffusion term in the Cahn-Hilliard equation. Accurate results are obtained provided the interfacial layer is resolved by at least four mesh cells and the Cahn number is ≤ 0.01. The coupling of the phase-field method with the single-field Navier-Stokes equation with surface tension term is validated by the drop deformation in shear flow. Simulations for a droplet on a smooth solid surface demonstrate the ability of the method to describe capillary-driven spreading processes caused by a mismatch of the initial and equilibrium contact angle for various values of the surface wettability.

1 Introduction

The spreading of liquid droplets on solid surface is a crucial process in many industrial applications, such as coating and painting, lubrication, ink-jet printing, adhesives and insecticides, oil recovery from porous rock, and reacting two-phase flows in chemical sponge reactors, etc. In addition to the fundamental issue of whether a liquid wets a given solid, many of these industrial applications require precise knowledge of the manner in which physical properties of the bulk flow and solid surface influence the spreading dynamics. To gain these insights, CFD can be a valuable tool.

In order to carry out reliable CFD simulations of the dynamic spreading process, it is vital to accurately model the motion of the contact line where the two-phase flow is in contact with the solid surface. In this context, conventional sharp-interface two-phase hydrodynamic models suffer from a paradox between the moving contact line and the no-slip boundary condition at the solid wall [1]. The latter leads to a stress singularity at the moving contact line where continuum fluid mechanics breaks down at the molecular length scales involved. To resolve this problem, various methods have been proposed (e.g., the precursor model [2] and the slip model [3]).

Among the various methods for interfacial simulations of two-phase flows [4], the phase field method is probably the most promising approach for handling moving contact lines. It is a diffuse interface method that treats the interface between two immiscible fluids as a transition region of small but finite width, endowed with surface tension [5]. Based on fluid free energy instead of force, the method can be traced to van der Waals a century ago [6]. Originally employed to model the initial stages of spinodal decomposition [7], the phase field method has become popular just in recent years as a numerical technique for simulating two-phase flows with a wide range of hydrodynamic and interfacial phenomena [8]. In our study, the most significant feature of this method is that it resolves the stress singularity at solid wall via a diffusive mechanism induced by a chemical potential gradient [9]. In addition to this advantage, the phase field method has other merits. First, from a computational perspective, modeling fluid interfaces as having finite thickness greatly simplifies the handing of topological transition of interfaces. Thus, this method has been successfully used to model breakup and coalescence of droplets [10]. Second, due to the energy-based formulation, it is straightforward to treat interfacial dynamics and rheology in a unified framework and thus to describe two-phase flows of complex non-Newtonian fluids [11]. Third, as an interface-capturing method, the phase field method treats the interface as a diffuse layer in a physical sense. It is distinct from other interface-capturing methods (e.g. the Volume-of-fluid and Level-set method) where the interface is sharp conceptually but handled as a diffuse layer by numerical regularization [12]. Thus in the phase field method, the modeling of interface is built on a rational physical basis and the artificial numerical efforts for interface regularization are reduced.

Alongside with these advantages, several issues inherent to the phase field method have to be handled carefully for numerical simulation. First, sufficient mesh resolution is needed to resolve the interface with finite thickness and thus to accurately capture interfacial phenomena there. Second, for numerical simulation with acceptable computational cost, the interface thickness is chosen with reference to the mean flow geometry rather than from that in real physics (which is usually of the order of nanometer). Thus it is necessary to investigate the influence of the interface thickness choice on the flow field. Third, as the motion of contact lines is driven by a diffusive process, it is critical to identify a suitable value/range for the diffusion coefficient and study the sensitivity of the spreading process with respect to this coefficient.

In this paper, we present our work on the implementation of the phase field method in OpenFOAM®, its verification, and first applications for simulating the spreading of a droplet. The paper is organized as follows. In section 2 we introduce the mathematical formulation of the phase field method for two-phase flows of incompressible, viscous and isothermal fluids and give an overview on the implementation of the method in OpenFOAM®. In Section 3, we discuss test case results for verification of the diffusion term in the Cahn-Hilliard equation and for surface tension, and present first results for the capillary-driven spreading of a droplet on an ideally flat surface. In section 4 we provide conclusions and outline future work.

2 Mathematical formulation

2.1. The phase field method

For a two-phase flow of incompressible, viscous and isothermal fluids, we introduce an order parameter (C) to characterize the two different phases. C varies rapidly but smoothly in the thin interfacial layer and is uniform in the bulk phases where it takes distinct values C_A and C_B; here we use $C_A = 1$ and $C_B = -1$. The transition layer from C_A to C_B represents the interfacial region. This binary fluid system is modeled by a Helmholtz free energy F which has the following form [6]

$$F = \int_V \left(\frac{1}{2}\alpha(\nabla C)^2 + \beta \Psi(C) \right) \mathrm{d}V \tag{1}$$

where V is the system domain. The first term accounts for the interfacial energy density and the second one is the bulk energy density. Ψ is a double-well potential function and is set conventionally as $\Psi = (1/4)(C+1)^2(C-1)^2$. α and β are two positive model constants. The chemical potential Φ is defined as the variational derivative of the free energy F with respect to the order parameter[1]:

$$\phi = \frac{\delta F}{\delta C} = \beta \Psi'(C) - \alpha \nabla^2 C \tag{2}$$

We can obtain the equilibrium interface profiles by minimizing F, i.e., solving $\Phi(C) = 0$. So its solutions are the equilibrium profiles: $C_A = 1$ and $C_B = -1$ that represent the two bulk phases and a one-dimensional (say, along the x-direction) non-uniform solution for the interface:

$$C_e = \tanh\left(\frac{x}{\sqrt{2}\xi} \right) \tag{3}$$

where $\xi = (\alpha/\beta)^{0.5}$ is the mean field thickness. We define the equilibrium interface thickness ε as the distance from $C = -0.9$ to $C = 0.9$, so that $\varepsilon = 2(2)^{0.5}\,\xi \tanh^{-1}(0.9) = 4.164\xi$. This width contains 98.5% of the surface tension stress [5]. In equilibrium, the surface tension σ equals to the integral of the free energy density along the interface [13]:

$$\sigma = \alpha \int_{-\infty}^{\infty} \left(\frac{\mathrm{d}C_e}{\mathrm{d}x} \right)^2 \mathrm{d}x = \frac{2\sqrt{2}}{3}\sqrt{\alpha\beta} \tag{4}$$

---

[1] In this paper we use the prime symbol to denote the first derivative of a function with respect to the order parameter C.

Thus the interface thickness ε and the surface tension σ can be controlled through the parameters α and β.

Cahn and Hilliard [14, 15] extended the problem to time-dependent situations by approximating interfacial diffusion to be proportional to chemical potential gradients, i.e., the Cahn-Hilliard equation:

$$\frac{\partial C}{\partial t} + (\mathbf{u} \cdot \nabla) C = \kappa \nabla^2 \phi \tag{5}$$

where $\mathbf{u}$ is the velocity field. The term on the right-hand-side of Eq. (5) accounts for a diffusive flux of the chemical potential gradient, where the mobility κ is a numerical parameter that controls the diffusion process. This diffusive mechanism serves to resolve the paradox between the moving contact line and the no-slip boundary condition at the solid wall. By making the assumption that the interface at the wall is at or near local equilibrium as the liquid wets the solid, a Neumann boundary condition for C is derived as follows:

$$\hat{\mathbf{n}}_s \cdot \nabla C = -\frac{\sigma \cos \theta_e}{\alpha} g'(C) \tag{6}$$

where $g(C) = 0.5 - 0.75C + 0.25C^3$ is a smoothly varying function that is equal to 0 for phase *A* ($C_A = 1$) and 1 for phase *B* ($C_B = -1$). θ_e is the equilibrium (static) contact angle. The wettability of the solid substrate is represented by the value of θ_e.

2.2. The equations of fluid motion

The single-field Navier-Stokes equations for the incompressible two-phase flow can be expressed as follows:

$$\nabla \cdot \mathbf{u} = 0 \tag{7}$$

$$\rho \left(\frac{\partial \mathbf{u}}{\partial t} + (\mathbf{u} \cdot \nabla) \mathbf{u} \right) = -\nabla p + \nabla \cdot (\mu (\nabla \mathbf{u} + \nabla \mathbf{u}^{\mathrm{T}})) + \mathbf{f}_{\mathrm{st}} + \rho \mathbf{g} \tag{8}$$

Here, ρ is the density of the mixture and $\mathbf{g}$ is the gravitational acceleration. In the sequel, the two phases have always the same density and the gravitational force is neglected. The viscosity of the binary mixture is

$$\mu(C) = \frac{1}{2} \left(\mu_A (C+1) - \mu_B (C-1) \right) \tag{9}$$

where μ_A and μ_B are the viscosity of phase *A* and *B,* respectively. The surface tension force $\mathbf{f}_{\mathrm{st}}$ is expressed in a potential form by the order parameter and the chemical potential [5]:

$$\mathbf{f}_{\mathrm{st}} = -C \nabla \phi \tag{10}$$

2.3. Non-dimensional formulation

We define the following dimensionless variables:

$$x^* = \frac{x}{L}, \quad u^* = \frac{u}{U}, \quad t^* = \frac{tU}{L}, \quad p^* = \frac{pL}{\mu_A U}, \quad \mu^* = \frac{\mu}{\mu_A} \tag{11}$$

where L and U represent a characteristic length and velocity scale respectively. Dropping the asterisks, we have the following dimensionless system.

The chemical potential field is:

$$\phi = \Psi'(C) - Cn^2 \nabla^2 C \tag{12}$$

The Cahn-Hilliard equation reads:

$$\frac{\partial C}{\partial t} + (\mathbf{u} \cdot \nabla) C = \frac{1}{Pe_\kappa} \nabla^2 \phi \tag{13}$$

The Neumann boundary condition for the order parameter is converted into:

$$\hat{\mathbf{n}}_s \cdot \nabla C = -\frac{2\sqrt{2} \cos\theta_e}{3Cn} g'(C) \tag{14}$$

The dimensionless form of the Navier-Stokes equations is:

$$\nabla \cdot \mathbf{u} = 0 \tag{15}$$

$$Re\left(\frac{\partial \mathbf{u}}{\partial t} + (\mathbf{u} \cdot \nabla)\mathbf{u} \right) = -\nabla p + \mu \nabla^2 \mathbf{u} + \mathbf{f}_{st} \tag{16}$$

where the surface tension force is given by

$$\mathbf{f}_{st} = -\frac{1}{Ca \cdot Cn} C \nabla \phi \tag{17}$$

and the formulation for the mixture viscosity is:

$$\mu(C) = \frac{1}{2}\left((C+1) - \frac{\mu_B}{\mu_A}(C-1) \right) \tag{18}$$

The dimensionless numbers are the Reynolds number (Re), the Capillary number (Ca), the Peclet number (Pe_κ) and the Cahn number (Cn) defined as

$$Re = \frac{\rho_A L U}{\mu_A}, \quad Ca = \frac{2\sqrt{2}\mu_A U}{3\sigma}, \quad Pe_\kappa = \frac{2\sqrt{2} L U \xi}{3\kappa\sigma}, \quad Cn = \frac{\xi}{L} \tag{19}$$

The Reynolds number is the ratio between the inertial and viscous forces. The Capillary number indicates the ratio between the viscous and surface tension forces. The Peclet number expresses the ratio between the convective and diffusive transports of the order parameter. It incorporates the mobility κ and thus is used to quantify the diffusion process that governs the motion of contact lines. The Cahn number represents the ratio of interface thickness and characteristic macroscopic length scale.

As said before, we consider the mobility and interface thickness as numerical parameters rather than physical ones. In our non-dimensional equations, Pe_κ and Cn are, therefore, to be considered as numerical parameters as well. One goal of this paper is to identify suitable ranges for both quantities. For this purpose we study their influence on the solution of various test problems in Section 3.

2.4. Implementation in OpenFOAM®

For implementation of the phase field method in OpenFOAM® we use the solver *icoDyMFoam* as starting point. The Cahn-Hilliard equation is added into the source code as a scalar transport equation. The convection term is implemented in an implicit and the diffusion term in an explicit manner. Due to its free energy formulation, the diffusion term consists of in-total fourth order derivative (see Eq. (12) and Eq. (13)). This is uncommon in usual transport equations in hydrodynamics and thus has not been dealt with in most OpenFOAM® applications. Here, we implement this term by substituting the chemical potential field into the Cahn-Hilliard equation. In the next section we shall present our verification work on this implementation. The surface tension force formulated from the order parameter and chemical potential is inserted as an explicit source term into the Navier-Stokes equation. In the implementation above, we use the linear (central differencing) interpolation scheme for the convection term, and the surface normal gradient scheme with explicit non-orthogonal correction for the Laplacian operators in the diffusion term. For time discretization we adopt the backward differencing scheme which is a second-order implicit method. The main procedure for advancing the solution from time-step n to $n+1$ is as follows:

(1) Update the chemical potential field using the order parameter field at time-step n according to Eq. (12).

(2) Obtain the order parameter at time-step $n+1$ by solving the Cahn-Hilliard equation (13) using the chemical potential from step (1) and the velocity field at time-step n.

(3) Compute the surface tension force according to Eq. (17) and the mixture viscosity by Eq. (18) using the order parameter at time-step $n+1$.

(4) Obtain the velocity field at time-step $n+1$ by solving the Navier-Stokes equations given by Eq. (15) and Eq. (16) with the PISO algorithm.

3 Verification and Validation by Test Problems

3.1. Verification on the diffusion term

As stated previously, we need to verify our implementation of the diffusion term. It is carried out by a one-dimensional test for a flat interface to solve the following equation without the convection term

$$\frac{\partial C}{\partial t} = \nabla^2 \left(\psi'(C) - Cn^2 \nabla^2 C \right) \tag{20}$$

The final equilibrium simulation results for C are compared with the respective analytical solution given by Eq. (3).

We run this simulation on a 1D domain of dimensionless length 1 with three different mesh resolutions: Δx=0.02, Δx=0.01 and Δx=0.005. The non-dimensional thickness of the interfacial region is $\varepsilon = 0.04164$. The number of cells in the interfacial region $N_C = \varepsilon/\Delta x$ then varies from 2 to 8 for the different grids. As shown in Figure 1, good agreement between the numerical and analytical solution is achieved supposed the interfacial region is resolved by at least 4 mesh cells.

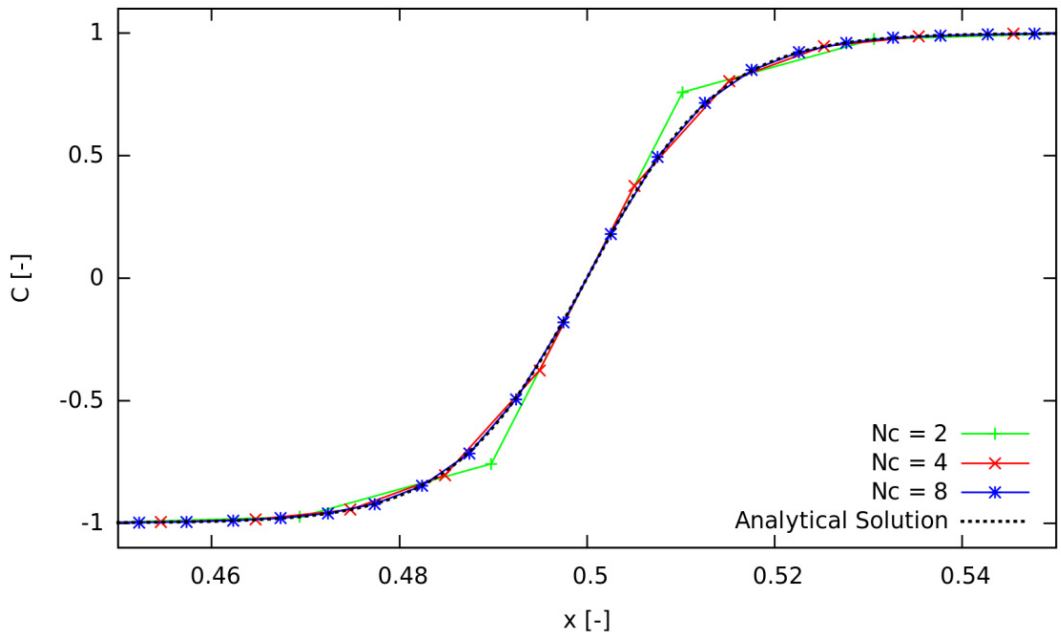

Figure 1: Comparison between analytical and computed equilibrium order parameter profile across the diffuse interface region for three different grids. The Cahn number is $Cn = 0.01$.

Next we extend our verification to a 2D test. Physically, the order parameter C should be in the range $[-1, 1]$. However, from the 2D simulation we get a field of the order parameter in the range $[-1+\Delta C, 1+\Delta C]$ with a shift $\Delta C=0.0052$ (Figure 2a). Yue et al. [16] found that this shift is related to the dimensionless interface thickness, namely the Cahn number (Cn). It is a phenomenon inherent to 2D or 3D modeling of the phase field method. By theoretical analysis, they gave for 2D problem the following linear relation:

$$\Delta C = \frac{\sqrt{2}}{3} Cn \tag{21}$$

To verify this analysis, we carry out numerical simulations using different values of Cn. Figure 2b shows a very good agreement between numerical and theoretical results. As Cn is getting smaller, the order parameter shift decreases and the upper and lower bounds are approaching the physical ones. This is desirable for guaranteeing mass conservation of the droplet. On the other hand, as Cn accounts for the interface thickness, it is not supposed to be too small otherwise a very fine mesh would be required to resolve this very thin interface. To make a compromise between accuracy and computational cost, $Cn=0.01$ is chosen in all the following simulations.

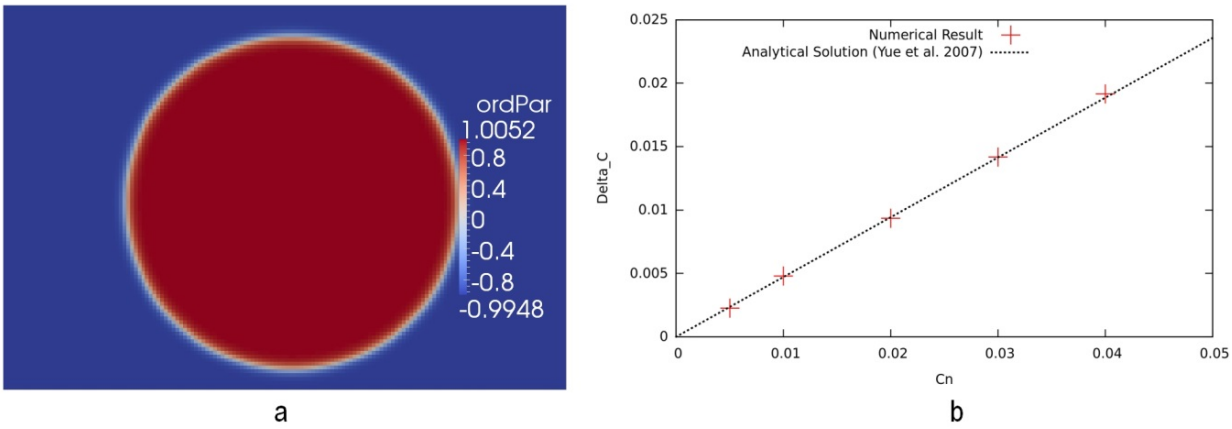

Figure 2: (a) the order parameter field from the 2D simulation; (b) comparison between the simulation results and the analytical solution on the relation between the Cahn Number (Cn) and the shift of the order parameter (ΔC).

3.2. Droplet deformation in an unbounded shear flow

In the phase field method the surface tension force is formulated in a potential form. This is different from other interface-capturing methods that represent this force by the interface curvature [17]. So here we verify and validate the implementation of the surface tension force in the Navier-Stokes equation. To achieve, this we consider a 2D problem: due to a shear flow, an initially spherical droplet deforms to an elliptic one (as shown in Figure 3). For this flow scenario, Taylor [18] gave an analytical solution that relates the deformation parameter (D) to the Capillary number (Ca)

$$D = 0.58Ca \tag{22}$$

This analytical solution[2] is derived based on the assumptions of creeping flow, same viscosity and density of the two phases and an unbounded domain.

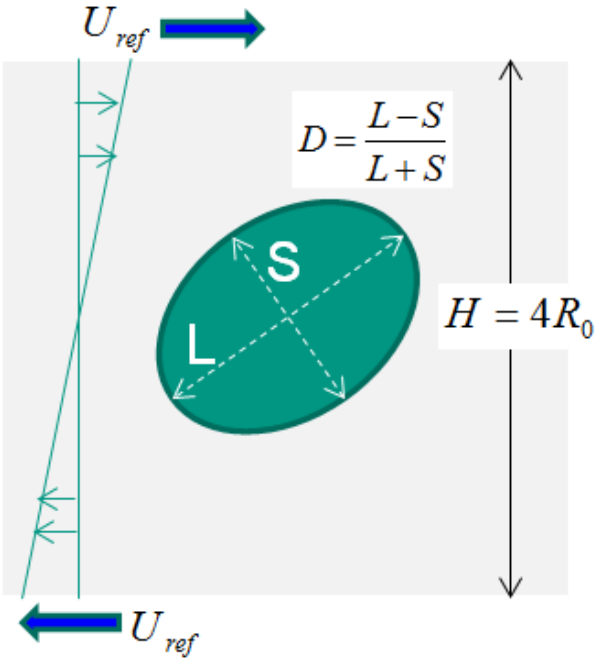

Figure 3: Sketch of the deformation of an initially spherical droplet to an ellipsoid shape in a shear flow.

[2] In Taylor's original paper, the capillary number is formulated using the shear rate and initial droplet radius. Here, the formula is adapted for the definition of the capillary number used in this work.

The droplet deformation simulation is started from the steady state of a precursor simulation where the Cahn-Hilliard equation is solved without convection term in order to reach an equilibrium state of C with a hyperbolic tangent profile across the interface. This calculation is carried out in a similar manner to the 2D test for the verification on the diffusion term. Due to the energy-based formalism of the phase field method, this preliminary simulation is necessary since it provides an order parameter field of complete saturation as an initial condition for further computation. This strategy is also adopted in [19].

Based on the initial condition above, we start the primary simulations by imposing a shear flow via setting the dimensionless velocities at the top and bottom boundary to $+1$ and -1 respectively. In Figure 4 we compare the numerical results for various values of Re and Ca with Taylor's analytical solution. For fixed values of Re, an almost linear relation between Ca and D is found. As Re decreases and approaches 0, the simulation results are converging to Taylor's analytical solution. This is reasonable since the analytical solution is made based on the creeping (Stokes) flow assumption where Re is assumed to be 0.

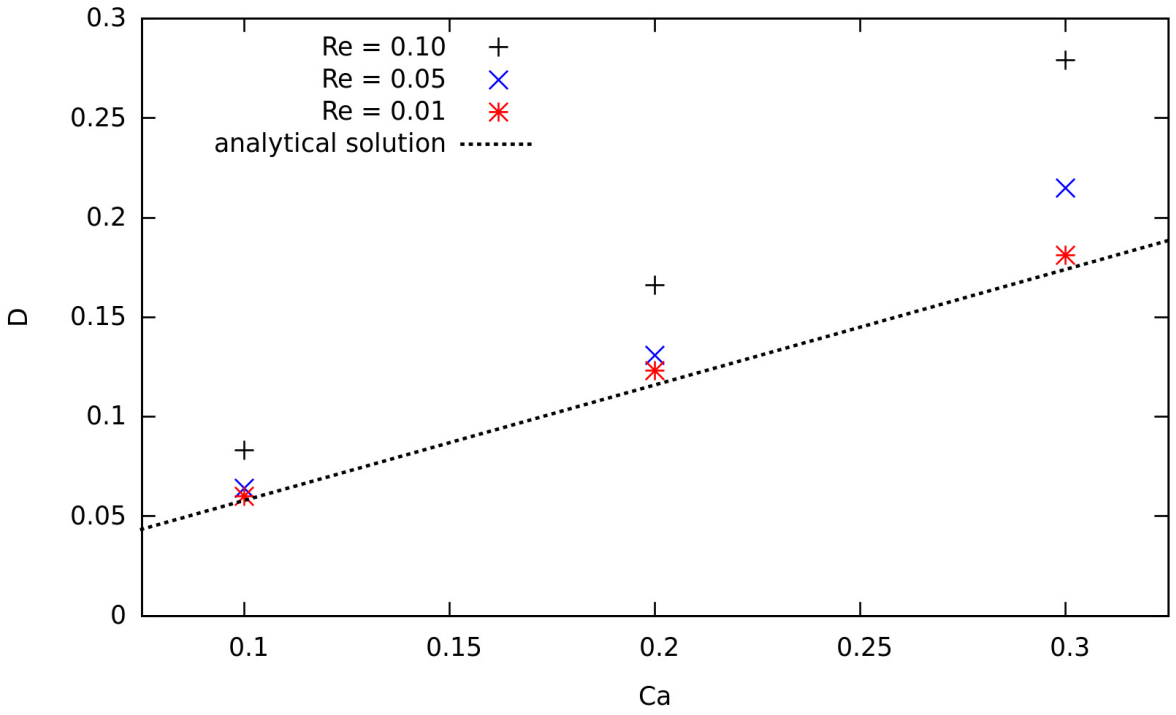

Figure 4: Comparison between the numerical results and Taylor's analytical solution for the relation between the Capillary number Ca and the deformation parameter D.

3.3. Droplet spreading on a flat surface

We perform a 2D simulation of the spreading of a droplet over a flat surface. The spreading is driven by capillary force while gravitational effect is assumed to be negligible. We use this test case to validate the ability of the implemented phase field method to adequately describe capillary flows and moving contact lines.

We run this simulation on a rectangular domain of dimensionless size 4×2. The mesh resolution is Δx=0.01 so that there are 4 cells to resolve the interface layer. The time-step size is set as $\Delta t = 0.001$. The maximal CFL number is around 0.002.

On the bottom solid wall, no-slip boundary condition is set for velocity and zero-gradient for pressure while the Neumann boundary condition for order parameter is set according to Eq. (14) with the help of the functionality *groovyBC*. For the outlets of the domain, zero-gradient boundary condition is set to both velocity and order parameter while pressure is specified as 0. The initial condition for the order parameter field is provided by the precursor calculation as described before.

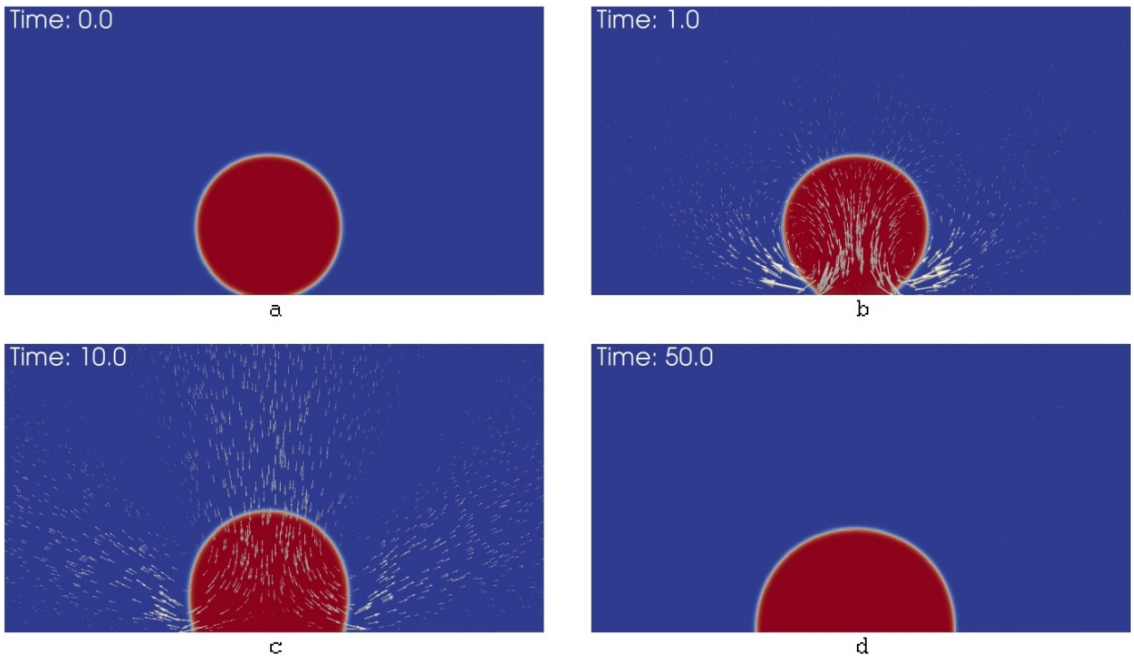

Figure 5: Simulation results for the capillary-driven spreading of a droplet on a horizontal flat surface for different instants in time. The dimensionless parameters are set as: $Re = 1.0$, $Ca = 1.0$, $Pe_\kappa = 1000$, $Cn = 0.01$. Both phases have the same viscosity. The initial and equilibrium contact angles are $\theta_0 = 155°$ and $\theta_e = 90°$ respectively. The white arrows represent the velocity field.

The computation is started from fluids at rest and a droplet with an initial contact angle θ_0=155°, see Figure 5a. The equilibrium contact angle is set to $\theta_e = 90°$ which is specified as boundary condition. Due to the mismatch between θ_0 and θ_e, the droplet begins to spread and the actual contact angle converges to θ_e. From the hydrodynamic theory, the driving force for the spreading is the interface-curvature-induced capillary force that overcomes the viscous resistance of the ambient fluid exerted on the droplet. At the first stage of spreading (Figure 5b), contact lines are moving fast, which brings about strong flow vortices nearby. Yet the global shape of the droplet has not been influenced and the droplet height remains almost stationary. At later stage (Figure 5c), the global shape is experiencing a noticeable change with a rapid decline of the droplet height. It leads to a strong downward flow. Meanwhile the largest vortices appear away from the contact lines and gradually dissipate while the droplet is slowly spreading to the final equilibrium state (Figure 5d), where the capillary force is in balance with the viscous resistance. The final contact angle agrees well with the specified equilibrium value. Similar spreading behaviors and flow fields are also reported in literature (e.g. [20-22]).

As mentioned previously, the motion of contact lines on the solid wall is governed by a diffusion process. So it is essential to make a sensible choice of the diffusion coefficient, that is, the Peclet number (Pe_κ). In the spreading simulation above, we chose $Pe_\kappa = 1000$. This choice is made with guidance from Jacqmin [5] who pointed out that the flow would be stagnant if the diffusion completely dominates the convection; on the other hand, if the diffusion is too small compared to the convection, the interface would be thinned or thickened by the flow. Through theoretical analysis, he gave the mobility parameter κ a limit $[O(\xi^2), O(\xi)]$. Equivalently, Pe_κ should be within the range $[O(10^2), O(10^4)]$ in this work. To substantiate this theoretical limit, two extreme cases with $Pe_\kappa = 50$ and $Pe_\kappa = 20000$ are run. The results agree well with the theoretical prediction (Figure 6): if Pe_κ is too small, diffusion overwhelms convection, thereby stalling the spreading process (Figure 6a). By contrast, when Pe_κ exceeds the upper limit, diffusion is damped by convection, the interface profile near the contact lines is noticeably deformed by the strong flows there (Figure 6b). In this way, $Pe_\kappa = 1000$ is selected as an appropriate value.

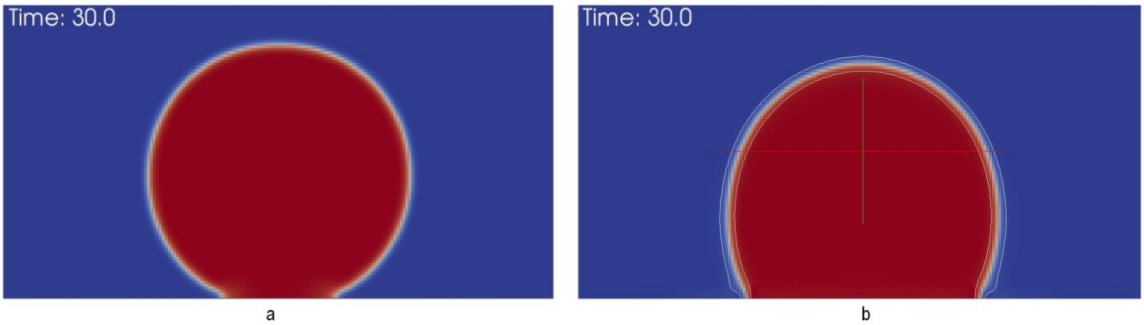

Figure 6: Numerical Simulations with two extreme Peclet numbers: (a) $Pe_\kappa = 50$; (b) $Pe_\kappa = 20000$, where the two contour lines denote $C = -0.9$ and $C = 0.9$ respectively. In both cases we use $Re = 1.0$, $Ca = 1.0$, $Cn = 0.01$, $\mu_B/\mu_A = 1.0$, $\theta_0 = 155°$, $\theta_e = 90°$.

Within the verified theoretical range, we carry out a sensitivity study on the influence of Pe_κ in the spreading behavior, see Figure 7. Here we investigate the spreading behavior by examining the temporal evolution of the droplet's base radius at the solid wall. It is found that as Pe_κ decreases, the base radius is changing faster which indicates a more rapid spreading of the droplet. This can be rationalized by the fact that the motion of contact lines is supported by the diffusion process. A stronger diffusion by setting a smaller Pe_κ drives a higher moving speed of the contact lines and thus a faster spreading of the droplet.

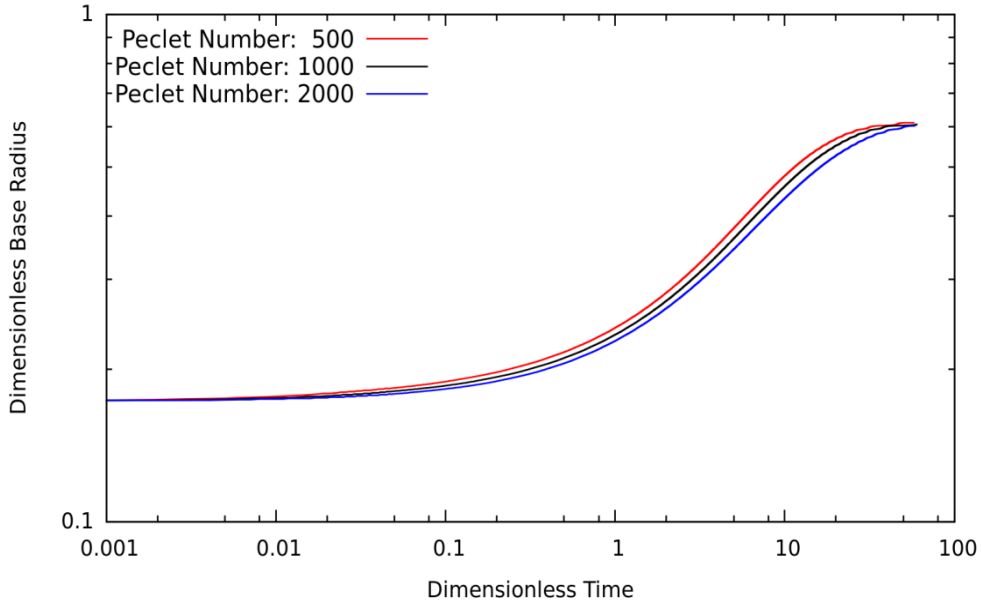

Figure 7: Temporal evolution of the droplet's base radius for different values of Pe_κ and $Re = 1.0$, $Ca = 1.0$, $Cn = 0.01$, $\mu_B/\mu_A = 1.0$, $\theta_0 = 155°$, $\theta_e = 90°$.

3.4. Effects of ambient fluid viscosity and substrate wettability on spreading behavior

With the implemented method, we investigate the effects of the ambient fluid viscosity and of the surface substrate wettability on the spreading rate, respectively.

First we perform the viscosity study by decreasing the viscosity ratio μ_B/μ_A from 1 to 0.5 and 0.25, where μ_A is the viscosity of the droplet and μ_B that of the ambient fluid. Since the viscosity of the droplet is fixed, the viscosity of the ambient fluid is getting smaller equivalently. As shown in Figure 8, a smaller viscosity of the ambient fluid leads to a faster spreading of the droplet. This trend is also reported in literature (e.g. [23]). This phenomenon is valid in terms of the hydrodynamics theory that as the ambient fluid is getting less viscous, its viscous resistance on the droplet spreading is reduced and thus the spreading is accelerated.

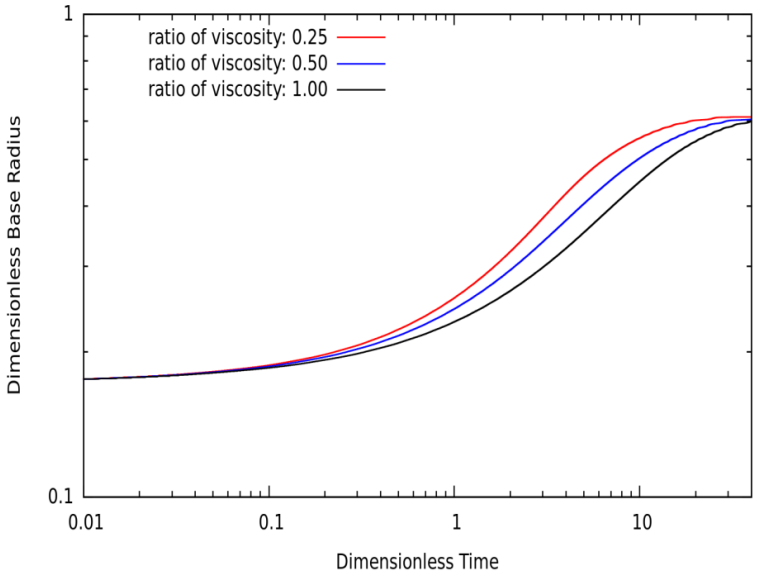

Figure 8: Temporal evolution of the droplet's base radius for different viscosity ratios and $Re = 1.0$, $Ca = 1.0$, $Cn = 0.01$, $Pe_\kappa = 1000$, $\theta_0 = 155°$, $\theta_e = 90°$.

The effect of substrate wettability is studied by using other two equilibrium contact angles ($\theta_e = 60°$ and $\theta_e = 120°$) according to the boundary condition Eq. (14). As Figure 9a shows, all the simulations predict accurately the final equilibrium contact angles. Looking at Figure 9b, we find that the spreading behavior is very sensitive to the substrate wettability from the very beginning. This finding agrees well with that reported in [22].

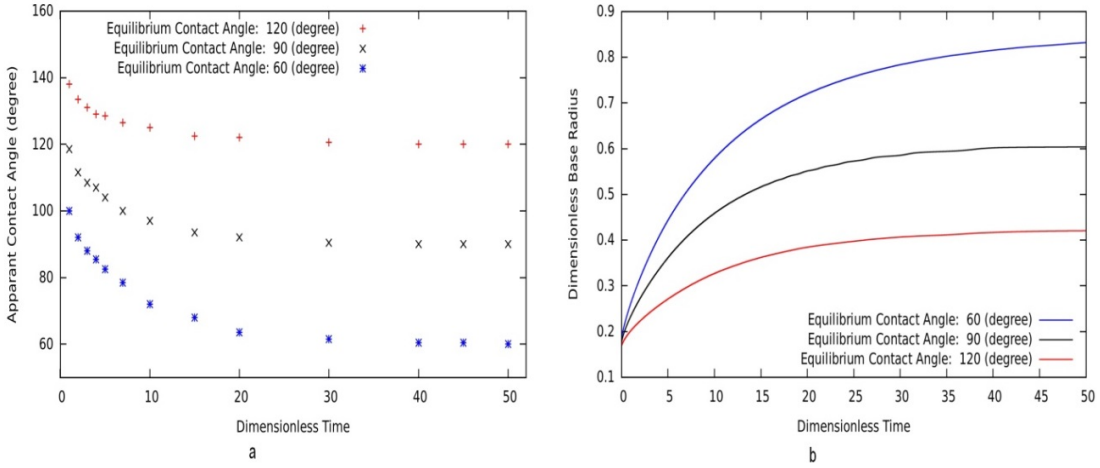

Figure 9: Temporal evolution of the apparent contact angle (a) and base radius (b) for different values of θ_e and $Re = 1.0$, $Ca = 1.0$, $Pe_\kappa = 1000$, $Cn = 0.01$, $\mu_B/\mu_A = 1.0$, $\theta_0 = 155°$.

4 Conclusions and future work

In this work a phase field method is implemented in OpenFOAM®. The method is carefully verified and validated by several test problems. The influence of various numerical parameters is investigated and the following conclusions can be drawn:

1. The computed one-dimensional profile of the order parameter in the interfacial region is in good agreement with the analytical solution supposed the interface thickness is resolved by at least four mesh cells.
2. For two-dimensional problems, the shift in the order parameter is negligible supposed the value of the Cahn number is below about 0.01.
3. The phase field method can reliably predict the deformation of a droplet in a shear flow which serves as validation for the surface tension force.
4. The method can successfully compute the spreading of a droplet on a solid surface driven by a mismatch between the initial contact angle and the specified equilibrium contact angle toward the steady state. The temporal evolution of this process slightly depends on the Peclet number. For the latter a suitable range has been identified.

As the next step we will further validate the method by comparing the predicted temporal evolution of base radius and contact angle using adaptive grids with experimental data. Up to now, we have investigated capillarity-driven spreading on ideally flat horizontal surfaces. In future we will also study spreading behavior driven by gravitational force by taking into account density difference between the two phases on inclined surfaces. The ultimate goal is to investigate spreading processes in more complex geometries as existing in solid sponges which are innovative chemical reactors.

Acknowledgement

We gratefully acknowledge the funding of this project by Helmholtz Energy Alliance “Energy-efficient chemical multiphase processes” (HA-E-0004).

References

[1] C. Huh, L.E. Scriven, Hydrodynamic Model of Steady Movement of a Solid/Liquid/Fluid Contact Line, J Colloid Interf Sci, 35 (1971) 85-100.

[2] P.G. de Gennes, Wetting - Statics and Dynamics, Rev Mod Phys, 57 (1985) 827-863.

[3] M. Renardy, Y. Renardy, J. Li, Numerical Simulation of Moving Contact Line Problems Using a Volume-of-Fluid Method, Journal of Computational Physics, 171 (2001) 243-263.

[4] M. Wörner, Numerical modeling of multiphase flows in microfluidics and micro process engineering: a review of methods and applications, Microfluidics and Nanofluidics, 12 (2012) 841-886.

[5] D. Jacqmin, Calculation of Two-Phase Navier-Stokes Flows Using Phase-Field Modeling, Journal of Computational Physics, 155 (1999) 96-127.

[6] J.D. van der Waals, The thermodynamic theory of capillarity under the hypothesis of a continuous variation of density (in Dutch), Verhandel/Konink Akad Weten, 1 (1879) 8.

[7] J.W. Cahn, Phase Separation by Spinodal Decomposition in Isotropic Systems, J Chem Phys, 42 (1965) 93-99.

[8] D.M. Anderson, G.B. McFadden, A.A. Wheeler, Diffuse-interface methods in fluid mechanics, Annual Review of Fluid Mechanics, 30 (1998) 139-165.

[9] D. Jacqmin, Contact-line dynamics of a diffuse fluid interface, J Fluid Mech, 402 (2000) 57-88.

[10] J. Lowengrub, L. Truskinovsky, Quasi-incompressible Cahn-Hilliard fluids and topological transitions, Proceedings of the Royal Society of London Series a-Mathematical Physical and Engineering Sciences, 454 (1998) 2617-2654.

[11] P.T. Yue, J.J. Feng, C. Liu, J. Shen, A diffuse-interface method for simulating two-phase flows of complex fluids, J Fluid Mech, 515 (2004) 293-317.

[12] P. Yue, C. Zhou, J.J. Feng, C.F. Ollivier-Gooch, H.H. Hu, Phase-field simulations of interfacial dynamics in viscoelastic fluids using finite elements with adaptive meshing, Journal of Computational Physics, 219 (2006) 47-67.

[13] A.J. Bray, Theory of Phase-Ordering Kinetics, Adv Phys, 43 (1994) 357-459.

[14] J.W. Cahn, J.E. Hilliard, Free Energy of a Nonuniform System I. Interfacial Free Energy, J Chem Phys, 28 (1958) 258-267.

[15] J.W. Cahn, J.E. Hilliard, Free Energy of a Nonuniform System III. Nucleation in a 2-Component Incompressible Fluid, J Chem Phys, 31 (1959) 688-699.

[16] P. Yue, C. Zhou, J.J. Feng, Spontaneous shrinkage of drops and mass conservation in phase-field simulations, Journal of Computational Physics, 223 (2007) 1-9.

[17] J.U. Brackbill, D.B. Kothe, C. Zemach, A continuum method for modeling surface tension, Journal of Computational Physics, 100 (1992) 335-354.

[18] G. Taylor, The formation of emulsions in definable fields of flow, Proceedings of the Royal Society of London. Series A, 146 (1934) 501-523.

[19] V.E. Badalassi, H.D. Ceniceros, S. Banerjee, Computation of multiphase systems with phase field models, Journal of Computational Physics, 190 (2003) 371-397.

[20] W. Villanueva, G. Amberg, Some generic capillary-driven flows, International Journal of Multiphase Flow, 32 (2006) 1072-1086.

[21] S. Afkhami, S. Zaleski, M. Bussmann, A mesh-dependent model for applying dynamic contact angles to VOF simulations, Journal of Computational Physics, 228 (2009) 5370-5389.

[22] V.V. Khatavkar, P.D. Anderson, H.E.H. Meijer, Capillary spreading of a droplet in the partially wetting regime using a diffuse-interface model, J Fluid Mech, 572 (2007) 367-387.

[23] H. Alla, S. Freifer, T. Roques-Carmes, A computational fluid dynamics model using the volume of fluid method for describing the dynamics of spreading of Newtonian fluids, Colloids and Surfaces A: Physicochemical and Engineering Aspects, 386 (2011) 107-115.